Oncogene (2007), 1–12

www.nature.com/onc

ORIGINAL ARTICLE

Phosphorylation of nm23-H1 by CKI induces its complex formation with h-prune and promotes cell motility

L Garzia[1], A D'Angelo[1], A Amoresano[2], SK Knauer[3], C Cirulli[2], C Campanella[4], RH Stauber[3,5], C Steegborn[6], A Iolascon[1] and M Zollo[1,7]

[1]CEINGE, Centro di Ingegneria Genetica e Biotecnologie Avanzate, Naples, Italy; [2]Dipartimento di Chimica Organica e Biochimica, Complesso Universitario Monte S. Angelo, Università degli Studi di Napoli 'Federico II', Naples, Italy; [3]Georg-Speyer-Haus, Frankfurt, Germany; [4]Dipartimento di Biologia Strutturale e Funzionale, Università degli Studi di Napoli 'Federico II', Naples, Italy; [5]Department of Otorhinolaryngology, Laboratory of Molecular Tumour Biology, University Hospital of Mainz, Mainz, Germany; [6]Department of Physiological Chemistry, Ruhr-University Bochum, Bochum, Germany and [7]Dipartimento di Biochimica e Biotecnologie Mediche, Facoltà di Scienze Biotecnologiche, Università degli Studi di Napoli 'Federico II', Naples, Italy

The combination of an increase in the cAMP-phosphodiesterase activity of h-prune and its interaction with nm23-H1 have been shown to be key steps in the induction of cellular motility in breast cancer cells. Here we present the molecular mechanisms of this interaction. The region of the nm23–h-prune interaction lies between S120 and S125 of nm23, where missense mutants show impaired binding; this region has been highly conserved throughout evolution, and can undergo serine phosphorylation by casein kinase I. Thus, the casein kinase I δ-ε specific inhibitor IC261 impairs the formation of the nm23–h-prune complex, which translates '*in vitro*' into inhibition of cellular motility in a breast cancer cellular model. A competitive permeable peptide containing the region for phosphorylation by casein kinase I impairs cellular motility to the same extent as IC261. The identification of these two modes of inhibition of formation of the nm23-H1–h-prune protein complex pave the way toward new challenges, including translational studies using IC261 or this competitive peptide '*in vivo*' to inhibit cellular motility induced by nm23-H1–h-prune complex formation during progression of breast cancer.

Oncogene advance online publication, 1 October 2007; doi:10.1038/sj.onc.1210822

Keywords: h-prune; nm23; CKI; motility; IC261

Introduction

The nm23 proteins have been conserved throughout evolution as they are ubiquitously expressed from bacteria to mammals. They possess a nucleoside diphosphate kinase (NDPK) activity that catalyzes transfer of the γ-phosphate from nucleoside triphosphates (NTPs) to NDPs. The human *nm23* gene family is composed of eight members, with *nm23-H1* having a high degree of homology (89%) to *nm23-H2*. *Nm23-H1* was identified as a metastasis suppressor gene (Steeg *et al*., 1988); in breast carcinoma, nm23 overexpression has been linked to early stages of the cancer, with loss of expression in more advanced cases. The human *nm23* genes have regulatory roles in cell proliferation, embryonic development, apoptosis, differentiation and tumor metastasis (Lacombe *et al*., 2000; Lascu, 2000). However, the NDPK activity alone cannot explain these pleomorphic effects. The nm23 proteins have been reported to possess both a histidine protein kinase activity and a phosphotransferase activity; the latter potentially represents an additional mechanism by which the nm23s can influence the metastasis and differentiation processes (MacDonald *et al*., 1996; Wagner *et al*., 1997). To date, several nm23 interactors have been described in mammals, including Rad, Tiam1, Arf6, the nucleosome assembly protein SET, Cdc42, EBNA1 and KSR (Otsuki *et al*., 2001; Tseng *et al*., 2001; Palacios *et al*., 2002), although their roles are not fully understood. AMPKa1, a heterotrimeric kinase that is a sensor of cellular energy status, binds to and phosphorylates nm23-H1, which in turn channels the ATP produced by its enzymatic activity to AMP activated kinase (AMPK) (Crawford *et al*., 2005, 2006).

An additional partner of the nm23 protein is seen in h-prune, the human homolog of the *Drosophila* prune protein (Reymond *et al*., 1999; Forus *et al*., 2001; D'Angelo *et al*., 2004). In *Drosophila*, a single copy mutation of proline 97 to serine in the *awd* gene is lethal in the genetic background of the *prune* gene, which is known as the Killer-of-Prune phenotype. Together with h-prune, the *Drosophila* prune protein belongs to the DHH superfamily of phosphoesterases, which includes the RecJ nuclease and pyrophosphatases from bacteria and yeast (Aravind and Koonin, 1998).

We have previously shown that amplification of h-prune copy number induces cell proliferation in an established breast cancer cellular model (Reymond *et al*., 1999), and we showed that this occurs through its cAMP-phosphodiesterase (PDE) activity (D'Angelo *et al*., 2004). Additionally,

Correspondence: Professor M Zollo, Molecular Oncology and Functional NeuroGenomics, CEINGE, Centro di Ingegneria Genetica e Biotecnologia Avanzate, Via Comunale Margherita 482, Naples 80131, Italy.
E-mail: zollo@ceinge.unina.it
Received 17 July 2006; revised 9 August 2007; accepted 28 August 2007

gene expression profile analyses have been indicating how several genes involved in cell motility are upregulated in the MDA-MB-435 c100 breast cancer models (D'Angelo and Zollo, 2004; Steeg, 2005). H-prune overexpression and nm23-H1–h-prune complex formation have a positive influence on cell motility, which suggests a role for h-prune in metastasis formation (D'Angelo and Zollo, 2004). In our first analyses on a large set of breast tumors, the pro-motility effects seen *in vitro* translated *in vivo* to significant association with lymph node status and metastasis formation, thus indicating that h-prune provides a new marker of advanced stage disease in breast carcinoma (Zollo *et al*., 2005).

It has been previously shown that *in vitro* nm23-H1 and nm23-H2 can be phosphorylated on S122 by casein kinase II (CKII) (Engel *et al*., 1994; Biondi *et al*., 1996), thus affecting their NDPK activity; additionally, the *Drosophila* protein with the S122A substitution is not phosphorylated. It is known that the mammalian CKI isoforms (α, β1, β2, γ1, γ2, δ, ε) can phosphorylate many different substrates, among which there are key regulatory proteins involved in control of cell proliferation and differentiation, crucial events during cancer progression (Knippschild *et al*., 2005).

We demonstrate here that the S122 and S125 serine residues of nm23-H1 and nm23-H2 are phosphorylated by CKI. Further, the specific CKIδ-ε inhibitor IC261 and our specific permeable peptide that mimics the nm23-H1 region of interaction with h-prune both disrupt the formation of the nm23-H1–h-prune protein complex. This results in inhibition of cell motility effects mediated via h-prune overexpression. These data have the potential to be used for 'translational studies' *in vivo* to reduce metastases formation arising from h-prune overexpression.

Results

Mapping the region of interaction between nm23-H1 and h-prune

Here, we first aimed to identify the interaction region between h-prune and nm23. An affinity chromatography approach was applied that uses the purified recombinant h-prune protein. Nm23-H1 cDNA was fragmented into four overlapping regions (see Materials and methods) and transfected into COS-7A cells; the protein extracts from these were applied to a Ni-NTA affinity column on which the recombinant h-prune protein had been preadsorbed. The eluted fractions were then analysed by western blotting: the nm23 protein fragment denoted as 'region 4' bound to the full-length h-prune protein. This is a region highly conserved in other species (see Figures 1a–c); no binding was seen for regions 1 and 2 of nm23, and there was only a weak interaction for region 3. To verify the results of the immunoprecipitation in living mammalian cells, we used fluorescent protein translocation biosensors (Knauer and Stauber, 2005). This method uses a nucleolus translocation amino-acid sequence to translocate a protein into the nucleolus. If binding occurs with the expressed protein, the translocation biosensor will detect it in the nucleolus. We thus expressed three overlapping regions of the nm23-H1 protein as green fluorescent protein (GFP)-prey_mdm2 fusions (Figure 1d). As expected, upon co-expression in HeLa and 293 cells, the GFP-prey_mdm2 fusions localized to the cytoplasm and did not colocalize with the empty blue fluorescence protein (BFP) bait in the nucleolus (data not shown). Next, we expressed the open reading frame (ORF) of the h-prune protein in the context of the BFP-bait construct. Upon transfection, the p53-bait fusions were correctly tethered to the nucleolus. However, only GFP-prey_H1B and _H1C induced the cytoplasm-to-nucleus translocation of the h-prune_BFP-bait, indicative of an efficient *in vivo* protein interaction (Figures 1d and e). Notably, GFP-prey_H1C was not tethered completely to the nucleolus by the bait, while GFP-prey_H1B was, indicative of a weaker interaction of H1C with the h-prune protein. No translocation was seen with GFP-prey_H1A. Similar results were obtained in 293 cells (data not shown). Interestingly, this region is highly conserved in the nm23 proteins across other species. We thus cloned the nm23 homologs from *Danio rerio*, *Caenorhabditis elegans*, *Drosophila melanogaster* and *Xenopus laevis* and expressed them in COS-7A cells, with the extracted proteins used in immunoprecipitation assays (see Supplementary material, Supplementary Figures 1SA–D). Our results indicate that the carboxyl terminus of nm23-H1 (aa 113–152) is primarily responsible for its interaction with h-prune.

The nm23–h-prune interaction is due to serine phosphorylation of nm23

Through bioinformatic predictions, the nm23-H1 and nm23-H2 regions spanning from S120 to S125 have high probability scores for phosphorylation by CKI and CKII. Additionally, the serine residue in position 125 has a perfect match with the S(p)-x-x-S consensus pattern identified for CKI. Of note, the amino-terminal serine must be phosphorylated before the C-terminal serine residue is phosphorylated (Kuret *et al*., 1985; Fiol *et al*., 1988). The phosphorylation of nm23 has already been demonstrated, with S122 serine phosphorylation by CKII occurring *in vitro* (Engel *et al*., 1994). From our co-immunoprecipitation analyses, the single point mutations in positions S122 and S125 of nm23-H1 both impaired its interaction with h-prune (see Supplementary Figures 2SA–D). Conversely, a missense mutation in S44, a residue already seen to be phosphorylated in human nm23, did not impair the nm23–h-prune interaction (Reymond *et al*., 1999), thus indicating that if phosphorylation is involved in nm23–h-prune binding, it is specific to the S120-S125 stretch of nm23. Further, considering that the CKI phosphorylation mechanism requires serine prephosphorylation at the 'upstream' serine of the consensus sequence, these S120 or S122 serines should prime the phosphorylation in position S125, and this latter phosphorylation should, in turn, regulate the interaction of nm23 with h-prune. To test

these hypotheses, we performed '*in vitro*' phosphorylation assays using wild-type nm23-H1 (see Figures 2a–c) and standard mass spectrometry analysis (see Material and methods). We identified two phosphopeptides, one with a doubly charged m/z of 783.3 lost this phosphate group (49 Da as neutral loss) during collision-induced dissociation (CID), to form a doubly charged fragment with an m/z of 734.3. The specific multiple reaction monitoring (MRM) transition method (Q1 = 783.3 and Q3 = 734.3) was thus used to detect this phosphopeptide. The interpretation of the MS/MS spectrum of the precursor ion at m/z 783.3 led to reconstruction of the sequence NIIHGSDSVESAEK, corresponding to peptides 115–128 within the nm23-H1 protein sequence (Figure 2a). The mass difference indicated the occurrence of a phosphorylation site at the level of S122; S120 and S125 were unmodified. The spectral analysis revealed another doubly charged (2+) signal at m/z 823.27, identified as the same 115–128 peptide that was modified with two phosphate groups at levels of both S122 and S125, with no modifications seen on S120. The phosphomodification on S122 occurs outside of the consensus sequence, a phenomenon that has been described for other casein kinase substrates (Marin *et al*., 1994, 2003).

We then investigated the ability of different isoforms of CKI to phosphorylate nm23-H1 *in vitro* (see Material and methods) using the recombinant proteins listed in Figure 2b. The rates of phosphate incorporation ranged from 0.44 to 2.5 nmol per mg of recombinant casein kinase. A CKI control peptide showed incorporation levels from 20 to 100 nmol min^{-1} mg^{-1}. The stoichiometry of the phosphate incorporation for CKIε was calculated as 0.01 pmol phosphate per pmol nm23-H1 per min. For CKIδ, this value dropped to 0.002 pmol phosphate per pmol nm23-H1 per min. Thus, CKIε is more efficient in its ability to phosphorylate nm23, with CKIδ showing a lower incorporation rate. We also determined the kinetic parameters of the phosphorylation of nm23-H1 by CKIε and CKIδ, as illustrated in Figure 2c, where CKIε displayed a higher affinity (lower K_m; 0.14 μM) versus nm23-H1, as compared to CKIδ (3.38 μM).

The phosphorylated and nonphosphorylated forms of nm23 were then tested for their binding to recombinant h-prune in an *in vitro* binding assay. Here, the nm23–h-prune interaction occurred only with the wild-type nm23 protein that had been previously phosphorylated by CKI. All of the single mutations to S120, S122 and

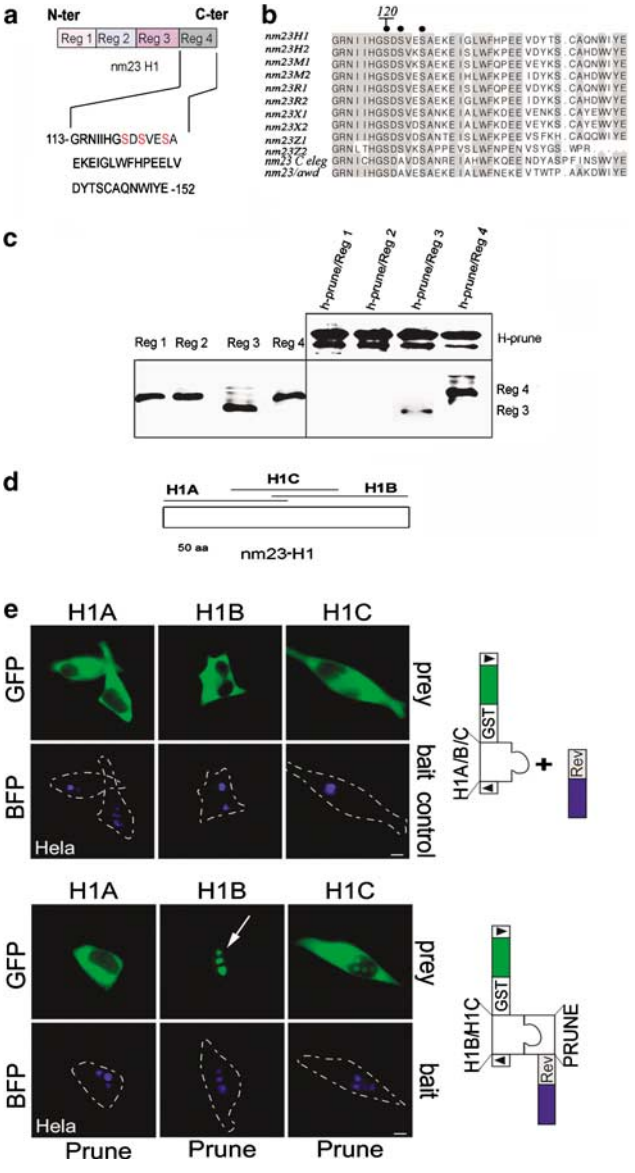

Figure 1 Mapping of the h-prune–nm23 interaction domain. (**a**) Schematic representation of the nm23 protein regions used in the *in vitro* immunoprecipitation assays. The sequence of region 4 that mediates the binding of nm23 with h-prune is shown. (**b**) Alignment of region 4 of nm23-H1 in different species. Gray shading shows residue identity between different species. The three serine residues, S120, S122 and S125, are strongly conserved (black dots). (**c**) The HA-tagged nm23 protein fragments, cloned in an HA pcDNA vector, were used to map the h-prune interaction region. Left: western blotting of total cell lysates (20 μg) from COS-7A cells transfected with the constructs carrying the cDNAs coding for the different regions, revealed by an anti-HA monoclonal antibody (Roche, Basel, Switzerland). Right: 1 μg of 6 × His tagged h-prune recombinant protein was incubated with Ni-NTA agarose magnetic beads for 1 h. Then 40 μg of the total cell lysates (left panel) was incubated with h-prune linked to the magnetic beads. After washes, the elution was performed with imidazole and the eluates were tested for the presence of both h-prune and the nm23-H1 regions with the A59 polyclonal antibody (Apotech-Alexis.com) and the anti-HA monoclonal antibody (Roche), as indicated. (**d**) Schematic representation of the nm23 protein regions used in the *in vivo* PTB mapping protein interaction assay. Bar, 50 amino acids. (**e**) PTB-based mapping of the nm23-H1–h-prune protein interaction interface in living cells. HeLa cells co-expressing the indicated prey/bait proteins were analysed by fluorescence microscopy for GFP and BFP fusions. Upon co-expression, the GFP-prey_nm23-H1 fusions (H1A, B, C) localized to the cytoplasm and did not colocalize with the empty BFP-bait at the nucleolus. In contrast, co-expression of the nucleolar anchored h-prune fusion (h-prune_BFP-bait) recruited GFP-prey_H1B (aa 71–152) and GFP-prey_H1C (aa 41–82) to the nucleolus, indicative of an efficient *in vivo* protein interaction. No interaction was observed for the GFP-prey_H1A (aa 1–80). Representative images are shown, and similar results were observed in two independent experiments. Arrow marks nucleolus. Scale bars, 10 μm. ▶: NLS, ◀: NES.

S125 tested prevented the binding between nm23-H1 and h-prune (Figure 2d). Furthermore, to exclude the possibility that nm23 binding with h-prune is through a conformational change in nm23, instead of a change in its phosphorylation status, two other additional single mutations outside of the region identified here were tested: K128G and H135G. Neither of these mutations disrupted the binding of nm23-H1 with h-prune after its phosphorylation with CKIδ (Figure 2e). This thus indicates that we can exclude the possibility that other

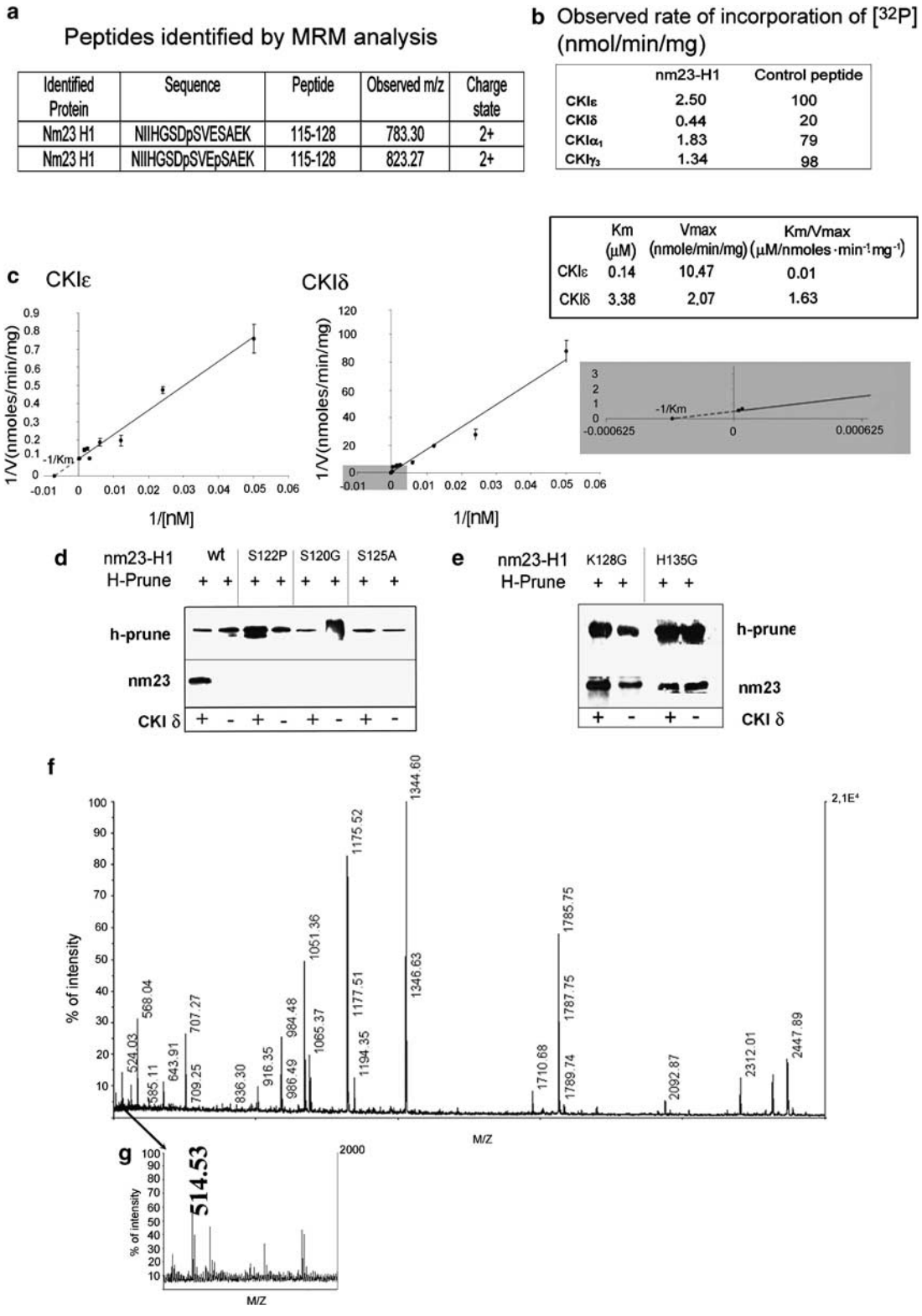

residues that affect the nm23 conformational status around this region are specifically involved with its h-prune interaction.

These findings do however suggest that the S120 residue is also necessary for nm23 binding with h-prune (Reymond *et al*., 1999), although the need for its phosphorylation was excluded in the interpretation of the MS/MS spectra, as summarized in Figure 2a. We believe that this is due to the transient nature of the phosphorylation of the S120 residue; nevertheless, this residue would appear to be important for the phosphorylation of the downstream S122 and S125 residues, and consequently for the interaction between nm23 and h-prune. Of note, while the data presented in Figures 2d and e relate specifically to the nm23-H1–h-prune interactions, identical results were obtained with nm23-H2 (data not shown).

Phosphorylation of nm23 occurs in the S120 to S125 region

Mass spectrometry analyses were used to detect the phosphorylation of these proteins when transiently expressed in living cells, followed by immunoprecipitation using an anti-HA-tag antibody. The immunoprecipitated HA-nm23-H2 protein was excised from SDS–polyacrylamide gel electrophoresis gels and analysed via tryptic digestion and matrix-assisted laser desorption/ionization–time of flight mass spectrometry. This indicated phosphorylation on S125 and on S122 or S120. Of note, the peptide at m/z 514.53 that contained both S120 and S122 showed an increase of 80 Da ($MW_{theoretical} =$ 434.53), which was thus only attributable to a single phosphorylation event (Figures 2f and g).

As it has been shown that S122 can be phosphorylated by CKII (Engel *et al*., 1994), here we cannot distinguish between phosphorylation on S120 or S122, although we do see S125 phosphorylation, and we believe that S122 phosphorylation can in turn promote phosphorylation on S125.

We also investigated whether nm23 phosphorylated by CKI was altered in terms of its oligomerization status and its NDPK activity, and how its oligomerization relates to its interaction with h-prune. Using the recombinant nm23 proteins expressed in *Escherichia coli*, the major proportion of nm23-H1 was normally present as a hexamer (39.7%) and a trimer (56.2%), although dimers (3.6%) and monomers (0.7%) were also detected (Figure 3a), as has been described previously (Kim *et al*., 2003). The data presented in Figure 3b show a significant increase in the hexameric structure upon CKI phosphorylation (hexamer, 53.6%; $P \leqslant 0.0015$; trimer, 42.2%; dimer, 4.1%; monomer, not detected; through gel filtration performed on the

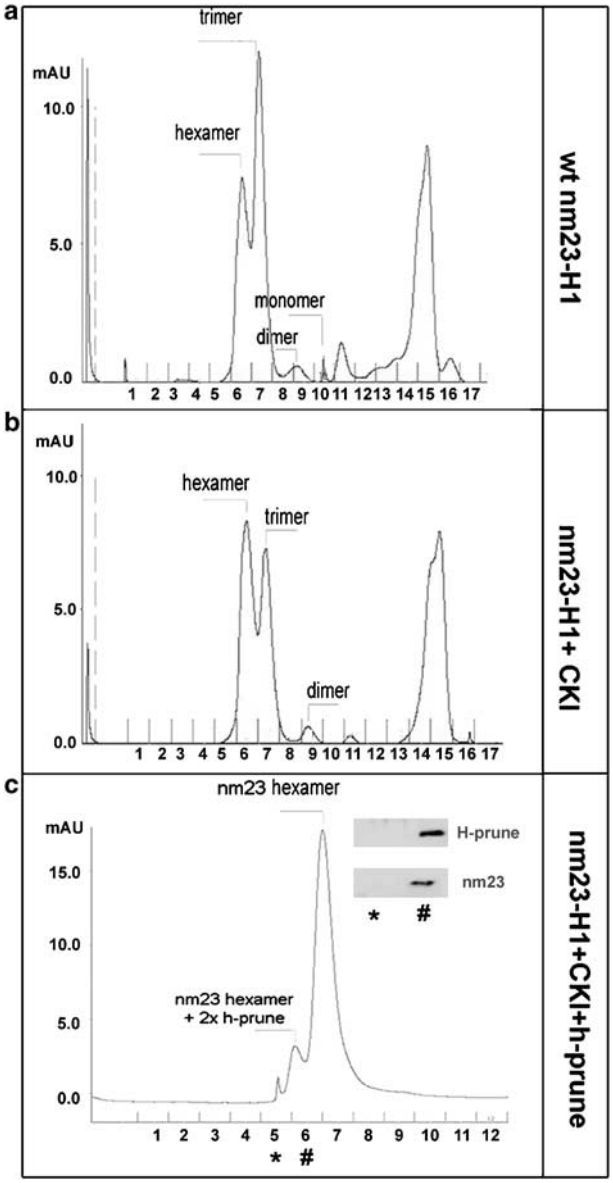

Figure 3 Influence of CKI phosphorylation on nm23 oligomerization. Multimeric structures formed by nm23-H1 in the absence (**a**) and presence of CKI treatment and without (**b**) or with (**c**) h-prune. Recombinant nm23-H1 was treated with CKI for 60 min at 30 °C. Hexamers, trimers, dimers and monomers are visible following gel filtration. $^{*}P \leqslant 0.001$; $^{\#}P \leqslant 0.002$; see also text.

Figure 2 The nm23–h-prune interaction depends on nm23 phosphorylation *in vitro*. (**a**) Nano-LC-mass spectrometry analysis of nm23-H1 after its *in vitro* phosphorylation by CKI. Two phosphopeptides were identified, one carrying one phosphorylation on S125 or two phosphorylations on S122 and S125. (**b**) Rates of incorporation of [^{32}P] in *in vitro* kinase assays using the CKI isoforms indicated, with nm23-H1 as a substrate. NB conducted with 0.1 mM ATP. (**c**) Lineweaver–Burke plots of the phosphorylation of nm23 by CKIε and CKIδ (10 min at 30 °C in the presence of 0.1 mM ATP), in gray is shown the intercept of the graph representing 1 km^{-1} of CKIδ. (**d–e**) *In vitro* binding assay using purified 6 × His-tagged h-prune expressed by the baculovirus system, using different 6 × His-tagged nm23-H1 protein mutants phosphorylated or not *in vitro* by the CKIδ recombinant protein. H-prune was immunoprecipitated with the A59 polyclonal antibody and both of the proteins were revealed in the pellet by an anti-His-tag antibody (Qiagen, Germantown, MD, USA). (**f**) MALDI spectrum of the nm23-H2 tryptic digest. (**g**) Enlarged portion of the MALDI spectrum of the nm23-H2 tryptic digest. The signal at m/z 514.53 was assigned to the tryptic fragment 140–143 carrying a phosphate group.

phosphorylated and nonphosphorylated nm23-H1 recombinant protein). Figure 3c shows the effects of addition of the recombinant h-prune protein to the reaction mixture. Here, a complex of h-prune and nm23 was eluted at 300 kDa, which was assigned to two molecules of h-prune and one hexamer of nm23. The two molecules of h-prune are present as a dimer, as additionally supported by recent findings (Middelhaufe *et al*., 2007). The presence of both proteins was also confirmed by western blotting using specific antibodies (Figure 3c). We also examined the effects of phosphorylation by CKI on the NDPK activity of nm23-H1 (Supplementary Figure 3S1). These results are reported in the Supplementary section, and they also support the preferential binding of h-prune to the hexameric form of nm23-H1.

The CKI-specific inhibitor IC261 impairs nm23 phosphorylation and its interaction with h-prune

To investigate regulation of nm23 phosphorylation *in vivo* and to determine to what extent this modification influences its complex formation with h-prune, we raised a polyclonal antibody in rabbit that preferentially recognizes the phosphorylated versus the nonphosphorylated forms of nm23. This was achieved by synthesizing a peptide with a sequence that corresponds to the region between N115 and E127 of nm23-H1 (see Materials and methods), and phosphorylated on S122. The antibody indeed specifically recognizes only phosphorylated nm23 (Figure 4a). A further characterize of the phosphoepitope antibody show that the S125A mutation completely abrogated the antibody reactivity, thus suggesting that the antibody preferentially recognizes the S125 phosphoepitope.

To date several CKI inhibitors are known (Rena *et al*., 2004), one of which is IC261, an ATP-competitive inhibitor that is selective for CKIδ and CKIε (Mashhoon *et al*., 2000). Other two known inhibitors are D4476 and CKI-7. While the selectivity of D4476 versus the CKI isoforms has not been defined, CKI-7 inhibitor is known to act on all CKI isoforms. This thus indicated the use of IC261, particularly considering its specificity toward CKIε and CKIδ.

The MDA-MB-435-c100 breast cancer cell line that constitutively expresses nm23-H1 (MDA-MB-H1-177) (Kantor *et al*., 1993) was thus treated with IC261, and total cell lysates were analysed by western blotting. As illustrated in Figure 4c, after 6–8 h of incubation with IC261 (see also Materials and methods; Cooper and Lampe (2002) and Li *et al*. (2004)), the signal intensity of nm23 phosphorylation decreased by 65% (quantified by imaging scan analyses; data not shown). To confirm any effects of inhibition of CKI on nm23 phosphorylation in cells and to avoid any misinterpretation relating to the relatively high levels of IC261 used (see below), here we also treated the MDA-MB-H1-177 cells with the two additional CKI inhibitors indicated above: D4476 and CKI-7 (Figure 4d). These results indicate that (i) the turnover of nm23-H1 and nm23-H2 phosphorylation by CKI is very low, and it appears that nm23 is largely constitutively phosphorylated in living cells (Figures 4c–e); (ii) these selective inhibitors for CKI abolish the phosphorylation of nm23 in the region within N115 to E127 (Figures 4c and d).

In these assays, IC261 was used at a concentration of 50 μM, CKI-7 at 400 μM, and D4476 at 25 μM, according to the concentrations reported in the literature (Cooper and Lampe, 2002; Izeradjene *et al*., 2004; Li *et al*., 2004; Rena *et al*., 2004).

To investigate the specificity of this phosphorylation and its inhibition further, we next used a specific inhibitor of CKII, 2-dimethylamino-4,5,6,7-tetrabromo-1H-benzimidazole (DMAT) (Pagano *et al*., 2004). When we treated the MDA-MB-H1-177 cells with DMAT, no effects were seen on the levels of phosphorylation of nm23-H1 (Figure 4e), which also provided further support for the specificity of our phosphoepitope antibody, in its specific recognition of the phosphorylation occurring on serines S122 and S125 of nm23 promoted by CKI. Then, to exclude possible side effects of the CKI inhibitors above versus cellular kinases such as AMPK and protein kinase A (PKA), we tested whether specific inhibitors of these kinases would also affect the phosphorylation of nm23. Here we used compound C and KT5720 with independent treatments at 20 and 10 μM, respectively (see literature data reported by Kim *et al*., 2002 and Lee *et al*., 2003), used with MDA-MB-H1-177 cells; neither of these kinase inhibitors affected the amounts of nm23 and phosphorylated nm23 revealed with the phosphoepitope antibody (Figure 4f).

To address whether this phosphorylation of nm23 mediates its binding to h-prune, we treated the MDA-MB-435-c100 cells with IC261 for 6 h (a time-frame chosen from above; see Figure 4c). The subsequent co-immunoprecipitation analyses for nm23 and h-prune revealed that the interaction between these two endogenous proteins occurred only in the absence of IC261 (Figure 4g), demonstrating that nm23 phosphorylation is necessary for its complex formation with h-prune. In contrast to this loss of complex formation with IC261 treatment, the CKII inhibitor DMAT did not influence the nm23–h-prune binding properties in MDA-MB-435-c100 cells, as shown by immunoprecipitation assays (Figure 4h).

Of note, the use of a 6-h treatment of the MDA-MB-435-c100 cells with CKI-7 and D4476 also efficiently impaired the nm23–H-prune interaction (Figure 4i), at similar levels as seen for IC261, further confirming the role of CKI in the regulation of this interaction. These experiments with CKI inhibitors are also useful for the discrimination between the potential effects of trans-phosphorylation versus auto-phosphorylation; even if small levels of nm23 modification can be ascribed to auto-phosphorylation, this basal auto-phosphorylation is not enough to lead to the formation of revealable amounts of the nm23–h-prune protein complex, as in the presence of the CKI inhibitors the nm23–h-prune interaction is impaired. Finally we were able to detect both δ and ε CKI isoforms as nm23 binders (Supplementary Figures 2SE and F). Therefore, when coupled

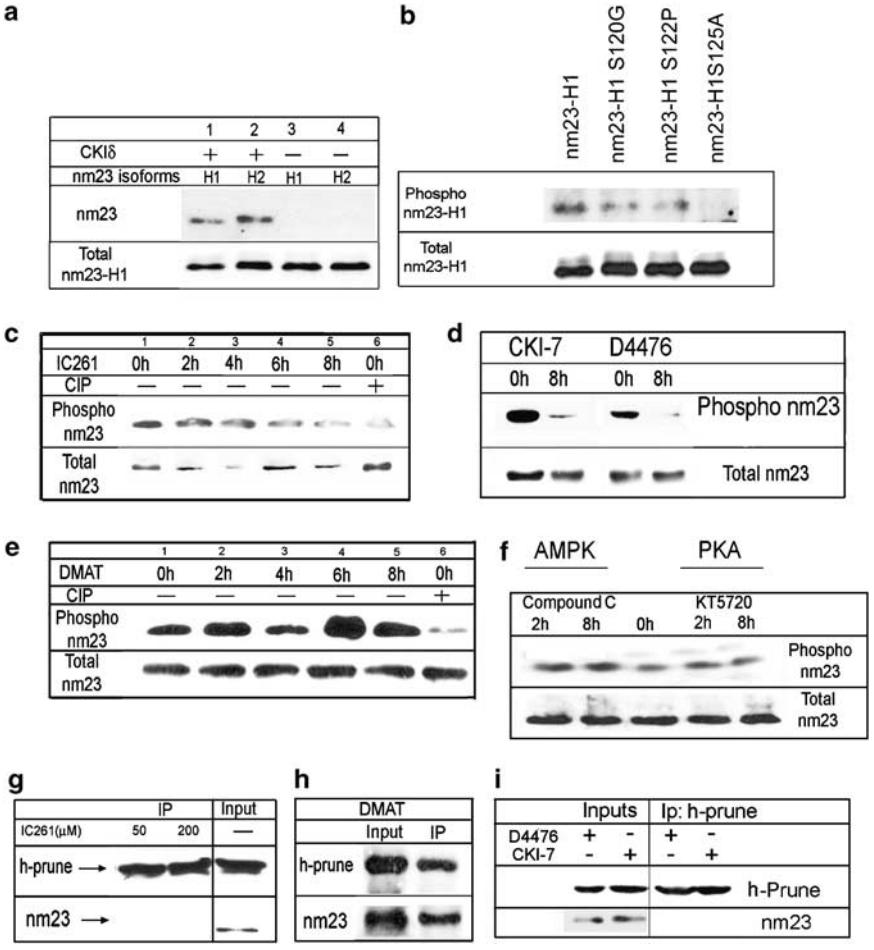

Figure 4 The nm23–h-prune interaction is impaired by IC261 in breast cancer cell lines. (**a**) Western blotting of recombinant nm23-H1 and nm23-H2 treated without and with recombinant CKIδ (as indicated). The K73 polyclonal anti-serum was affinity purified using the phosphorylated synthetic nm23 peptide used as immunogen. Total nm23 revealed by the unpurified K73 antibody. (**b**) The phosphoepitope antibody was tested by western blotting for its affinity versus the serine mutants of nm23: COS-7A cells were transfected with the indicated expression constructs and total cell lysates probed for immunoreactivity. Nm23-H1 S125A mutation abolishes the immunoreactivity. Total nm23 revealed by the unpurified K73 antibody. (**c**) The CKIε and CKIδ inhibitor IC261 blocks nm23-H1 phosphorylation *in vitro* in the MDA-MB-H1-177 clone overexpressing nm23-H1. Western blotting of MDA-MB-H1-177 cells treated with 50 μM IC261; total protein extracts analysed after 0, 2, 4, 6, 8 h of treatment for the presence of nm23 phosphorylation, using the affinity-purified K73 polyclonal antibody against the nm23 phosphorylated synthetic peptide. Lane 6: protein extracts pretreated with calf intestine phosphatase (CIP) as control. Bottom panel: total nm23 in the protein extracts used in the immunoprecipitation, using an anti-nm23-H1 monoclonal antibody (Santa Cruz, Santa Cruz, CA, USA). (**d**) As (**c**), with two additional inhibitors of CKI: 400 μM CKI-7 and 25 μM D4476, each for 8 h (chosen from the previous time course with IC261, considering the probably low turnover of the site). (**e**) As (**c**), with an inhibitor of CKII: 10 μM DMAT for 0, 2, 4, 6 and 8 h. (**f**) As (**c**), with inhibitors of AMPK and PKA, respectively: 20 μM compound C and 10 μM KT5720 for 2 and 8 h. (**g**) MDA-MB-435-c100 breast cancer cell line treated with IC261 for 6 h, as indicated. H-prune was immunoprecipitated from total cell lysates with the A59 polyclonal antibody. The interaction with nm23-H1 was revealed with an anti-nm23-H1 monoclonal antibody (Santa Cruz). (**h**) As (**g**), with an inhibitor of CKII: 10 μM DMAT for 2 h. Immunoprecipitation with an antibody for h-prune; immunoprecipitates were probed with the unpurified K73 to detect nm23 in the interaction. (**i**) As (**g**), with two additional inhibitors of CKI: 400 μM CKI-7 and 25 μM D4476, each for 8 h. Immunoprecipitation and probing as (**h**).

with the previous *in vitro* results shown in Figure 2b, these findings indicate CKIε as a strong candidate for the kinase that phosphorylates nm23 *in vivo*.

Inhibition of nm23–h-prune binding decreases motility of breast cancer cells

The enhanced cell motility induced by h-prune overexpression can be ascribed to two concurrent phenomena: first, an increase in cAMP-PDE activity, with a corresponding decrease in cAMP levels in the cells; and secondly, the formation of the h-prune and nm23 protein complex, which would reduce the amount of free nm23 in the cell, with nm23 known to be responsible for the suppression of motility (D'Angelo *et al*., 2004).

To test this hypothesis, we treated our MDA-MB-435-c100, h-prune-overexpressing, stable clones (MDA-MB-h-prune #3, #4) with IC261, both alone and together with dipyridamole (the selective h-prune cAMP-PDE inhibitor) (Figure 5a). In this cell-motility assay, the presence of IC261 alone substantially

decreased the serum-stimulated pro-motility effects of h-prune overexpression, without affecting that of the MDA-MB-435-c100 wild-type cells, thus indicating the specificity of this effect for cells that express high levels of h-prune (Figure 5a). As the wild-type cells also maintained their basal motility when stimulated with serum, this also indicates that this lowering of cell motility in the stable clones overexpressing h-prune is not due to a toxic side effect. Indeed, these cells remained viable after 6 h of treatment (as evaluated by trypan blue dye exclusion, data not shown). Of note, while the PDE inhibitor, dipyridamole also decreased the serum-stimulated pro-motility effects in these h-prune overexpressing clones, the addition of both the CKI and dipyridamole together did not lead to any additive effects in this cell motility assay system (Figure 5a). Furthermore, the addition of both IC261 and dipyridamole together at suboptimal levels did not lead to additive effects in their reduction of cell motility in these cells overexpressing h-prune (Figure 5b).

We also made use of the cell penetrating region of the HIV TAT protein. Here it was fused to a peptide containing the nm23 region phosphorylated by CKI. This peptide should be able to be phosphorylated by CKI and consequently to impair the phosphorylation of the wild-type nm23, thus preventing its interaction with h-prune see Materials and methods and literature data (Zhang *et al*., 2004).

To be certain of this mechanism, we first tested whether the peptide impaired phosphorylation of nm23 with CKI *in vitro*. Increasing amounts of the peptide did indeed lower the amount of nm23 phosphorylation by CKI in a phosphorylation reaction using [γ-^{32}P]-ATP (Figure 5c); in contrast, a scrambled peptide did not affect nm23 phosphorylation under the same conditions (Figure 5d). The specific peptide also impaired the nm23–h-prune interaction with treatment of the MDA-MB-h-prune #4 clone, as shown in co-immunoprecipitation assays (Figure 5e). Moreover, we also used this specific peptide (with the scrambled peptide control) to

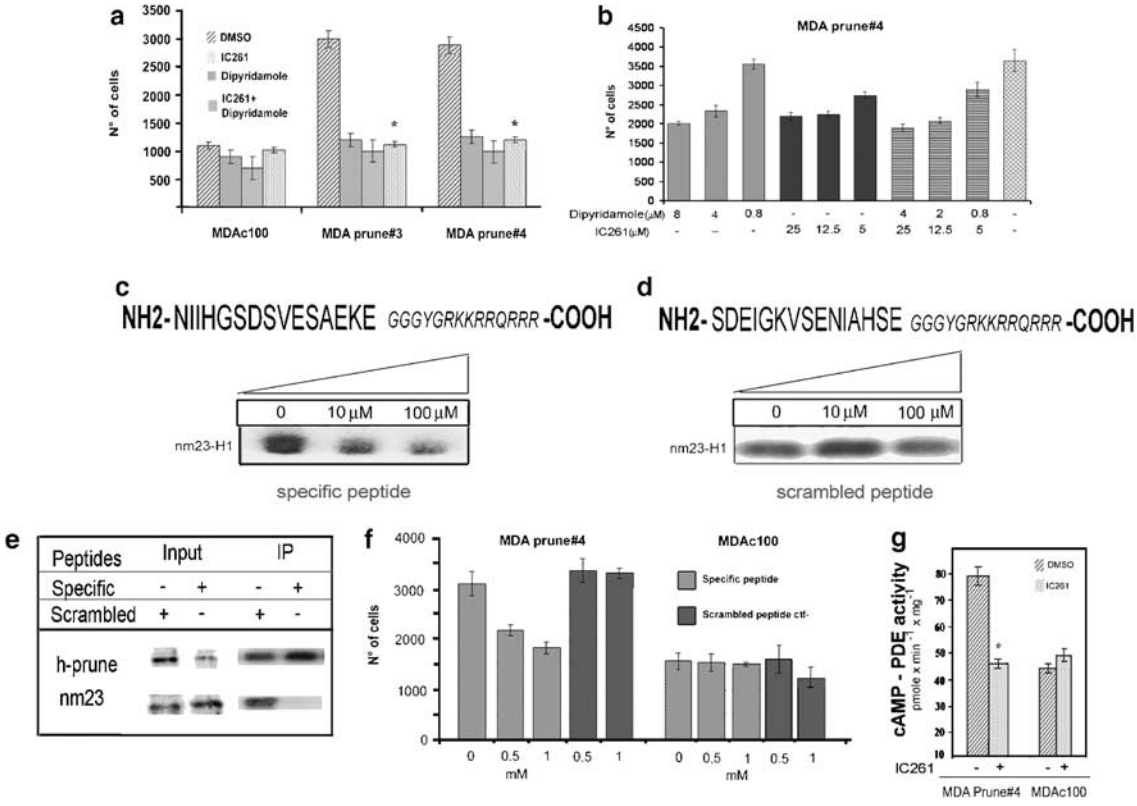

Figure 5 Inhibition of cell motility in MDA-MB-435 breast cancer cells overexpressing h-prune. (**a**) MDA-MB-435-c100 and stable h-prune-overexpressing MDA-MB-h-prune clones #3 and #4 cells treated with 50 μM IC261 and 8 μM dipyridamole, as indicated, for 8 and 24 h, respectively. A Boyden chamber-like cell motility assay was used in the presence of 0.5% FCS, expressed as number of cells counted under the microscope (means, ± s.d., from five independent experiments, each carried out in duplicate). *$P = 0.002$ (Student's *t*-test; MDA-MB-h-prune clones #3 and #4 versus MDA-MB-h-prune clones #3 and #4 with IC261). (**b**) As (**a**) with stable h-prune-overexpressing MDA-MB-h-prune clones #4 and suboptimal concentrations of IC261 and dipyridamole separately and together, as indicated. No significant additive effects were seen. (**c** and **d**) Effects of specific competitive cell-permeable peptide (**c**) and scrambled control peptide (**d**) on nm23-H1 phosphorylation. Nm23 was incubated with CKI and increasing amounts of the peptides, as indicated, and nm23-H1 phosphorylation was followed using [γ^{32}P]-ATP. (**e**) MDA-MB-435-c100 cells were treated with the indicated peptides for 24 h, with the cell extracts immunoprecipitated with the anti-h-prune polyclonal antibody. In the presence of the specific cell-permeant peptide, nm23 was not detectable in the immunoprecipitates, as revealed by the use of the unpurified K73 anti-nm23 antibody. (**f**) As (**a**), with MDA-MB-h-prune clone #4 and MDA-MB-435 c100 cells treated the specific and scrambled peptides. The specific cell-permeant peptide blocked the h-prune-overexpression-dependent cell motility in a dose-dependent manner. (**g**) PDE activity measured in total protein lysates from MDA-MB-h-prune clone #4 and MDA-MB-435 c100 cells treated with vehicle or with 50 μM IC261. *$P = 0.001$ (Student's *t*-test; MDA-MB-h-prune clone #4 versus MDA-MB-prune clone 4# treated with IC621).

treat the MDA-MB-435-c100 wild-type cells and the MDA-MB-h-prune #4 cells that were subsequently assayed for cell motility (as above). Here, with the specific peptide, the cell motility was reduced in the h-prune-overexpressing clone in a dose-dependent manner; neither the scrambled peptide nor the MDA-MB-435-c100 wild-type cells showed any effects (Figure 5f). This thus indicates that by specifically impairing nm23 phosphorylation, and consequently nm23–h-prune complex formation, by the use of this specific peptide, similar decreases in the motility of MDA-MB-h-prune #4 cells were seen when compared to the direct inhibition of CKI with IC261 (Figures 5a–f).

Taken together, these findings demonstrate the importance of the formation of the protein complex between h-prune and nm23 for the induction of cell motility and the potential to use these two independent agents to impair this process.

IC261 decreases the cAMP-PDE activity of the MDA-MB-h-prune overexpressing cells

To determine whether the IC261 inhibition of the cellular motility induced by h-prune overexpression is due to a direct inhibition of the h-prune cAMP-PDE activity, we initially tested this activity of the recombinant h-prune protein in the presence of IC261: the h-prune PDE activity was not affected (data not shown). Therefore, as it has been previously reported that the nm23–h-prune interaction can stimulate the h-prune PDE activity *in vitro* (D'Angelo and Zollo, 2004), we asked if IC261 treatment of the MDA-MB-h-prune #4 clone would inhibit h-prune PDE activity. These cells show an increased total cAMP-PDE activity over the MDA-MB-435-c100 wild-type cells (D'Angelo and Zollo, 2004). Indeed, here in the presence of IC261, the increase of total cAMP-PDE activity due to the h-prune overexpression in these MDA-MB-h-prune #4 cells was lost, while the total cAMP-PDE activity of the wild-type cells was not affected (see Figure 5g). This thus suggests that the nm23–h-prune interaction has a leading role in the h-prune cAMP-PDE activity in breast cancer cells. Of note, this disruption of the nm23–h-prune interaction also affects the cellular localization of h-prune, as described in the Supplementary material (see Supplementary Figures 4SA and B).

Discussion

Protein–protein interactions are essential processes that occur during cell homeostasis, leading to the formation of protein complexes within the networks of their actions. H-prune- and nm23-interacting proteins have been evolutionarily conserved in the vertebrate species, including *Homo sapiens, Mus musculus*, *D. rerio* and *X. laevis*. The principal finding of the present study is the regulation of nm23 in the cell environment as part of the CKI signaling cascade, whereby nm23 is phosphorylated by the CKI family, which results in the modulation of its interaction with h-prune. Nm23 and h-prune bind together through the nm23 C-terminal domain, where three independent point mutations in conserved serine residues impair the interaction.

When a recombinant CKI enzyme was used to phosphorylate nm23 *in vitro*, two modifications were detectable by MRM mass spectrometry analysis, S122 and S125. While S122 is a residue that is also phosphorylated by CKII *in vitro* on both nm23-H1 and nm23-H2, to date there have been no reports describing the phosphorylation on S125. Serine auto-phosphorylation mostly on S44, is accounting for only 0.2% of the total auto-phosphorylation (Bominaar *et al*., 1994). We have thus concluded that CKI is responsible for the S125 phosphorylation of nm23, as it is the only source of phosphate known for this residue, while for position S122, we cannot, at present, fully exclude a contribution of auto-phosphorylation. Through *in vitro* kinase assays we were also able to determine that all of the CKI isoforms tested, namely α1, δ, ε, γ3, can phosphorylate nm23-H1, with CKIε as the most active isoform on nm23-H1 (see Figures 2b and c).

In the context of the nm23–h-prune interaction, it appears that phosphorylation on S125, S122 and S120 are all necessary, because in the presence of individual point mutations in each of these residues the interactions with h-prune were impaired (Figure 2d). However, we found only two phosphorylated serines (S125, S122) *in vitro*, which suggests to us that the S120 modification occurs in a transient manner, and maybe for the priming of the phosphorylation of a downstream residue. Similarly, *in vivo* in mammalian cells, nm23-H2 (the more suitable protein to be analysed by triptic digestion) was phosphorylated on S125 and on either S120 or S122; again, transient phosphorylation on S120 cannot be excluded, and this phosphorylation could be important to enhance the acid context that is necessary for CKII phosphorylation on S122 (Meggio *et al*., 1993). A recent study has also shown that autophosphorylation of the nm23-H1-S120G protein corrected its folding defect (Mocan *et al*., 2007). But what fraction of the nm23 proteins is phosphorylated in living cells, and how is this fraction is regulated in response to different stimuli are still open questions.

We were not able to detect a change in nm23 phosphorylation status with CKII, AMPK or PKA inhibitors, and the CKII inhibitor DMAT did not impair the binding of nm23 with h-prune. However, it is of note that nm23-H1 phosphorylation on S122 by AMPKα1 has been reported as a way of regulating the interaction of these two proteins in liver (Crawford *et al*., 2006). As this appears contrary to the results presented in Figure 4f for AMPK inhibition here, we believe that this could be ascribed to the different cellular types and models used (that is, liver versus breast).

Our analyses with the use of IC261, has revealed that nm23 is constitutively phosphorylated by these kinases in breast cancer cells, thus providing an anti-motility activity in a breast cancer cell model (MDA-MB-435). The absence of an effect of IC261 on the wild-type MDA-MB-435-c100 breast cancer cell line (Figure 5a)

indicates that its effects are limited to an inhibition of cell motility induced by h-prune or by the formation of the nm23H1–h-prune complex. We chose the MDA-MB-h-prune #3 and MDA-MB-h-prune #4 cell lines that retain more balanced expression levels of the two proteins (nm23 and h-prune) as our model of cell motility induced by the formation of the nm23H1–h-prune complex (Figure 5a).

Figure 6 illustrates in summary our model of the function of the nm23H1–h-prune complex, where we hypothesize that the formation of this complex impairs the level of free nm23 that can function as an anti-metastatic protein, although this phenomenon represents only a part of the mechanisms beneath the increased cell motility induced by h-prune overexpression. Of note, the finding that IC261 fully blocks the increase in PDE activity induced by h-prune raised the possibility that the formation of the nm23–h-prune complex has a role in the cAMP-PDE enzymatic activity of h-prune. Indeed, it appears that IC261 decreases the h-prune PDE activity indirectly through its inhibition of h-prune binding to nm23, impairing the serine phosphorylation of nm23 and resulting in a lowering of the cell motility to the levels seen in the control MDA-MB-435-c100 wild-type cell line. Thus, the model proposed implies that the nm23–h-prune complex is formed to increase the activation of the h-prune cAMP-PDE activity (see model in Figure 6). This protein complex that is necessary for h-prune activity can, in turn, be regulated by the other proteins in the cellular context, possibly in terms of protein kinases or additional protein binders, which can control h-prune activity and which might also compete for h-prune binding with nm23. Thus, a question arises whether the effects of IC261 can be ascribed to direct or indirect actions against other pathways that take part in the regulation of several phosphodiesterases. We believe that this phenomenon possesses, at least in our experimental model, a level of specificity toward the formation of the nm23–h-prune protein complex and its induction of cell motility. The model proposed here involves only the h-prune protein complex with nm23-H1, and it does not fully unravel the relationship with the complex quaternary structure of nm23-H1, which is known to form homo-oligomers and hetero-oligomers (Heo *et al*., 1997). However, evidence reported here does show that h-prune binds the hexameric structures of nm23-H1, which is known to be correlated to its anti-motility function and negatively influenced by h-prune, and that this interaction is controlled by CKI phosphorylation.

An important biological function of the CKI family is a regulatory role in the Wnt/Frizzled/β-catenin pathway (Gao *et al*., 2002; Hino *et al*., 2003).

At this time, only the data reported by Kobayashi *et al*. (2006) and Garzia *et al*. (2006) link h-prune to GSK3-β, a protein involved in the *Wnt* activation pathway, and to cell migration. Our findings show that IC261 impairs cell motility, thus raising the hypothesis that h-prune, nm23 and CKIε, the last of which has already been found to be involved in the modulation of the signaling of dishevelled (Cong *et al*., 2004), have roles in the Wnt pathway. These hypotheses might thus open up new aspects of the migration-based mechanism that involves h-prune as an important actor and of the physiopathological functions of h-prune within the complex with nm23 in cancer metastasis formation.

Materials and methods

Plasmid construction and protein expression

The plasmids GFP-prey_H1A (nm23-H1 aa 1–80), GFP-prey_H1B (nm23-H1 aa 71–152), GFP-prey_H1C (nm23-H1 aa 41–82) encode three overlapping regions of the nm23-H1

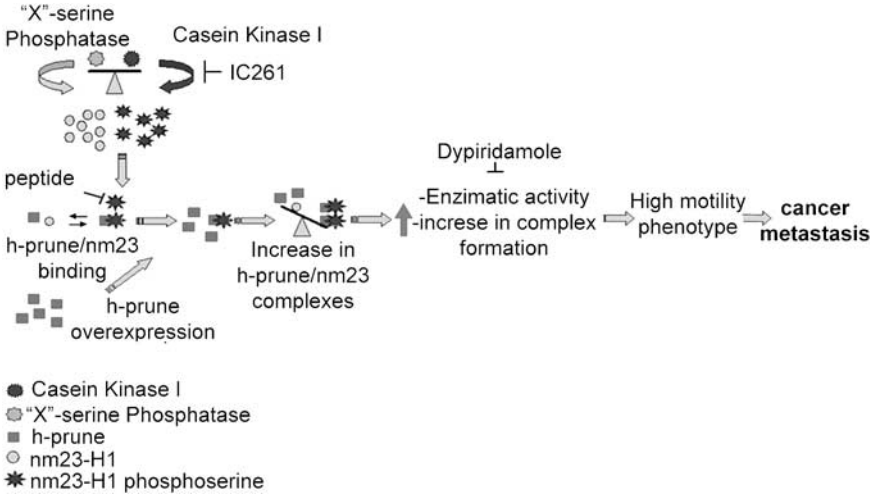

Figure 6 Model for the h-prune and nm23-H1 interactions in breast cancer cells overexpressing h-prune. CKI and an 'X' serine phosphatase factor are responsible for the balance between the amounts of the proteins in either a 'complex' or as 'noncomplexed'. The complex formation between h-prune and nm23 is one of the first events to occur together with h-prune overexpression, which leads to an increase in cell motility that is induced by the h-prune cAMP-PDE activity. Complex formation is necessary for the functional activation of h-prune cAMP-PDE. Three independent agents (IC261, the permeable peptide and dipyridamole) have been identified as inhibiting cancer progression upon h-prune overexpression.

protein as NLS-GFP/GST-nm23-H1-RevNES fusions. Plasmid p_prune-RevM10-BFP encodes a nucleolar anchored fusion protein composed of h-prune and a NES deficient HIV-1 Rev-BFP fusion (BFP-prune_bait) (Knauer and Stauber, 2005). Plasmids were constructed by PCR amplification and cloning into pNLS-GFP/GST-RevNES or pRevM10-BFP, as described previously (Knauer and Stauber, 2005).

Nm23 from *X. laevis* was obtained from total RNA that was extracted from unfertilized eggs using a standard reverse transcriptase–PCR protocol. The nm23-specific sequence was amplified with specific primers (available upon request) and cloned into the HA-pcDNA vector (Invitrogen, Carlsbad, CA, USA). The same strategy was applied to nm23 cloning from *D. rerio*, *C. elegans* and *D. melanogaster*, using total RNA from 48-h embryos, adult worms and adult flies, respectively. The cDNA coding for nm23-H1-S120G, and S122P and S125A were obtained through standard methods of site-directed mutagenesis on wild-type sequences cloned in HA-pCDNA and pFastBacHta vectors (Invitrogen), using the QuickChange III Kit (Stratagene, La Jolla, CA, USA). Cloning of human CKIδ and CKIε were performed by standard molecular biology protocols, with total RNA from HeLa cells retrotranscribed with iScript (Biorad, Hercules, CA, USA) following the manufacturer's protocol. CKIδ and CKIε were amplified by PCR with the following primers:

CKI-delta_eco_for CGGGAATTCATGGAGCTGAGAG TCGGGAACAG; CKI-delta_xho_rev CGGCTCGAGTCCT CGGTGCACGACAGACTG; and CKI-epsilon_hind_for CGGAAGCTTATGGAGCTACGTGTGGGGAACAAG; CKI-epsilon_hind_rev CGGAAGCTTTCGCTTCCCGAGATGGTC AAATGGC.

The cDNA were then inserted into the pReyzo expression vector digested with the appropriate restriction enzymes. The protein expression and purification of h-prune and wild-type nm23 and its mutants were performed with a baculovirus expression system (Invitrogen) and Ni-NTA affinity resin, as described previously (Garzia *et al*., 2003). Specific and scrambled cell penetrating peptides were synthesized by PRIMM (Milan, Italy); the sequences are shown in Figures 5c and d.

Gel filtration assay

Gel filtration assays were performed on an Atka FPLC system (Amersham Biosciences, Piscataway, NJ, USA) using an Amersham Biosciences Superdex 200 PC 3.2/30 column equilibrated and eluted in 50 mM Tris buffer, pH 7.5, containing 150 mM NaCl. Samples of nm23-H1 (50 μg) that were nonphosphorylated or were phosphorylated by CK1 kinase as described previously (Garzia *et al*., 2003) were dissolved in an appropriate volume of buffer to a final concentration of 10 μM. All experiments were carried out at 25 °C with a flow rate of 0.5 ml min^{-1}. The column was calibrated under the same conditions with proteins of known molecular mass: bovine albumin (66 kDa), carbonic anhydrase (30 kDa) and cytochrome C (11 kDa).

The nm23-H1 was then reduced in 300 mM Tris–HCl, pH 8.5, 1.25 mM EDTA, 6 M guanidinium chloride by incubation with dithiothreitol at a 10:1 molar excess over the total –SH groups (37 °C, 2 h, nitrogen atmosphere). The free cysteine residues were alkylated with iodoacetamide at a 5:1 molar excess over the total –SH groups (room temperature, 30 min, in the dark, nitrogen atmosphere). Excess of reagents were removed from protein samples by gel filtration on PD10 Sephadex G25 columns. Enzymatic digestion was carried out with trypsin in 50 mM ammonium bicarbonate, pH 8.5, at an enzyme:substrate ratio of 1:50 (w/w) (37 °C for 18 h).

PDE activity assay with cAMP as substrate

PDE activity was measured as described previously (D'Angelo *et al*., 2004). See also Supplementary material.

MALDI–TOF mass spectrometry, nanoLC-mass spectrometry, cell-based techniques, *in vitro* phosphorylation, interaction assays and phospho-nm23 antibody generation, are available as Supplementary material.

Acknowledgements

For fruitful discussions and critical reading of the manuscript, the authors would like to thank Professor Gennaro Marino, University of Biotechnology, Federico II, Naples (Italy). Additionally, we thank Dr Nadia De Marco (University of Science, Federico II, Naples, Italy) for supplying material for *Xenopus* cloning, Professor Massimo Lancieri (University of Science, Federico II, Naples, Italy) for Zebra fish material and cloning, and Dr Bazzicalupo (IGB-CNR, Naples, Italy) for the *C. elegans* nm23 material and cloning. We thank Dr Patricia Steeg (National Cancer Institute, Bethesda, MD, USA) for kindly providing us with the MDA-MB-MB345 c100 and H1 177 cell lines and Professor Lorenzo Pinna (University of Science, Padova, Italy) for providing us with DMAT, a specific CKII inhibitor. This work was supported by a 2005–2007 'AIRC-FIRC progetto regionale' grant (MZ), a FIRC fellowship (LG), the Open University (UK) TIGEM PhD Programme (LG), a FIRB-MIUR-RBAU01RW82 grant (MZ), EU BRECOSM-LSH-CT-503234 (RS, MZ) and EUFP6 EET-Pipeline (MZ) grants and an 'Associazione Italiana lotta al Neuroblastoma' grant (AI, MZ) 2006-2007.

References

Aravind L, Koonin EV. (1998). The HD domain defines a new superfamily of metal-dependent phosphohydrolases. *Trends Biochem Sci* **23**: 17–19.

Biondi RM, Engel M, Sauane M, Welter C, Issinger OG, Jimenez de Asua L *et al*. (1996). Inhibition of nucleoside diphosphate kinase activity by *in vitro* phosphorylation by protein kinase CK2. Differential phosphorylation of NDP kinases in HeLa cells in culture. *FEBS Lett* **399**: 183–187.

Bominaar AA, Tepper AD, Veron M. (1994). Autophosphorylation of nucleoside diphosphate kinase on non-histidine residues. *FEBS Lett* **353**: 5–8.

Cong F, Schweizer L, Varmus H. (2004). Casein kinase Iepsilon modulates the signaling specificities of dishevelled. *Mol Cell Biol* **24**: 2000–2011.

Cooper CD, Lampe PD. (2002). Casein kinase 1 regulates connexin-43 gap junction assembly. *J Biol Chem* **277**: 44962–44968.

Crawford RM, Treharne KJ, Arnaud-Dabernat S, Daniel JY, Foretz M, Viollet B *et al*. (2006). Understanding the molecular basis of the interaction between NDPK-A and AMPK alpha 1. *Mol Cell Biol* **15**: 5921–5931.

Crawford RM, Treharne KJ, Best OG, Muimo R, Riemen CE, Mehta A. (2005). A novel physical and functional association between nucleoside diphosphate kinase A and AMP-activated protein kinase alpha1 in liver and lung. *Biochem J* **392**: 201–209.

D'Angelo A, Garzia L, Andre A, Carotenuto P, Aglio V, Guardiola O *et al*. (2004). Prune cAMP phosphodiesterase binds nm23-H1 and promotes cancer metastasis. *Cancer Cell* **5**: 137–149.

D'Angelo A, Zollo M. (2004). Unraveling genes and pathways influenced by H-prune PDE overexpression: a model to study cellular motility. *Cell Cycle* **3**: 758–761.

Engel M, Issinger OG, Lascu I, Seib T, Dooley S, Zang KD *et al*. (1994). Phosphorylation of nm23/nucleoside diphosphate kinase by

casein kinase 2 *in vitro*. *Biochem Biophys Res Commun* **199**: 1041–1048.

Fiol CJ, Haseman JH, Wang YH, Roach PJ, Roeske RW, Kowalczuk M *et al*. (1988). Phosphoserine as a recognition determinant for glycogen synthase kinase-3: phosphorylation of a synthetic peptide based on the G-component of protein phosphatase-1. *Arch Biochem Biophys* **267**: 797–802.

Forus A, D'Angelo A, Henriksen J, Merla G, Maelandsmo GM, Florenes VA *et al*. (2001). Amplification and overexpression of PRUNE in human sarcomas and breast carcinomas—a possible mechanism for altering the nm23-H1 activity. *Oncogene* **20**: 6881–6890.

Gao ZH, Seeling JM, Hill V, Yochum A, Virshup DM. (2002). Casein kinase I phosphorylates and destabilizes the beta-catenin degradation complex. *Proc Natl Acad Sci USA* **99**: 1182–1187.

Garzia L, Andre A, Amoresano A, D'Angelo A, Martusciello R, Cirulli C *et al*. (2003). Method to express and purify nm23-H2 protein from baculovirus-infected cells. *Biotechniques* **35**: 384–388, 390–391.

Garzia L, Roma C, Tata N, Pagnozzi D, Pucci P, Zollo M. (2006). H-prune-nm23-H1 protein complex and correlation to pathways in cancer metastasis. *J Bioenerg Biomembr* **38**: 205–213.

Heo YJ, Kim SY, Kim E, Lee KJ. (1997). Quaternary structural analysis of nucleoside diphosphate kinases using capillary electrophoresis. *J Chromatogr A* **781**: 251–261.

Hino S, Michiue T, Asashima M, Kikuchi A. (2003). Casein kinase I epsilon enhances the binding of Dvl-1 to Frat-1 and is essential for Wnt-3a-induced accumulation of beta-catenin. *J Biol Chem* **278**: 14066–14073.

Izeradjene K, Douglas L, Delaney AB, Houghton JA. (2004). Casein kinase I attenuates tumor necrosis factor-related apoptosis-inducing ligand-induced apoptosis by regulating the recruitment of fas-associated death domain and procaspase-8 to the death-inducing signaling complex. *Cancer Res* **64**: 8036–8044.

Kantor JD, McCormick B, Steeg PS, Zetter BR. (1993). Inhibition of cell motility after nm23 transfection of human and murine tumor cells. *Cancer Res* **53**: 1971–1973.

Kim MS, Cheong YP, So HS, Lee KM, Son Y, Lee CS *et al*. (2002). Regulation of cyclic AMP-dependent response element-binding protein (CREB) by the nociceptin/orphanin FQ in human dopaminergic SH-SY5Y cells. *Biochem Biophys Res Commun* **291**: 663–668.

Kim YI, Park S, Jeoung DI, Lee H. (2003). Point mutations affecting the oligomeric structure of Nm23-H1 abrogates its inhibitory activity on colonization and invasion of prostate cancer cells. *Biochem Biophys Res Commun* **307**: 281–289.

Knauer SK, Stauber RH. (2005). Development of an autofluorescent translocation biosensor system to investigate protein-protein interactions in living cells. *Anal Chem* **77**: 4815–4820.

Knippschild U, Gocht A, Wolff S, Huber N, Lohler J, Stoter M. (2005). The casein kinase 1 family: participation in multiple cellular processes in eukaryotes. *Cell Signal* **17**: 675–689.

Kobayashi T, Hino S, Oue N, Asahara T, Zollo M, Yasui W *et al*. (2006). Glycogen synthase kinase 3 and h-prune regulate cell migration by modulating focal adhesions. *Mol Cell Biol* **26**: 898–911.

Kuret J, Woodgett JR, Cohen P. (1985). Multisite phosphorylation of glycogen synthase from rabbit skeletal muscle. Identification of the sites phosphorylated by casein kinase-I. *Eur J Biochem* **151**: 39–48.

Lacombe ML, Milon L, Munier A, Mehus JG, Lambeth DO. (2000). The human Nm23/nucleoside diphosphate kinases. *J Bioenerg Biomembr* **32**: 247–258.

Lascu L. (2000). Quaternary structure of nucleoside diphosphate kinases. *J Bioenerg Biomembr* **32**: 213–214.

Lee M, Hwang JT, Lee HJ, Jung SN, Kang I, Chi SG *et al*. (2003). AMP-activated protein kinase activity is critical for hypoxia-inducible factor-1 transcriptional activity and its target gene expression under hypoxic conditions in DU145 cells. *J Biol Chem* **278**: 39653–39661.

Li G, Yin H, Kuret J. (2004). Casein kinase 1 delta phosphorylates tau and disrupts its binding to microtubules. *J Biol Chem* **279**: 15938–15945.

MacDonald NJ, Freije JM, Stracke ML, Manrow RE, Steeg PS. (1996). Mutation of proline 96 or serine 120 abrogates its motility inhibitory activity upon transfection into human breast carcinoma cells. *J Biol Chem* **271**: 25107–25116.

Marin O, Bustos VH, Cesaro L, Meggio F, Pagano MA, Antonelli M *et al*. (2003). A noncanonical sequence phosphorylated by casein kinase 1 in beta-catenin may play a role in casein kinase 1 targeting of important signaling proteins. *Proc Natl Acad Sci USA* **100**: 10193–10200.

Marin O, Meggio F, Sarno S, Andretta M, Pinna LA. (1994). Phosphorylation of synthetic fragments of inhibitor-2 of protein phosphatase-1 by casein kinase-1 and -2. Evidence that phosphorylated residues are not strictly required for efficient targeting by casein kinase-1. *Eur J Biochem* **223**: 647–653.

Mashhoon N, DeMaggio AJ, Tereshko V, Bergmeier SC, Egli M, Hoekstra MF *et al*. (2000). Crystal structure of a conformation-selective casein kinase-1 inhibitor. *J Biol Chem* **275**: 20052–20060.

Meggio F, Boldyreff B, Issinger OG, Pinna LA. (1993). The autophosphorylation and p34cdc2 phosphorylation sites of casein kinase-2 beta-subunit are not essential for reconstituting the fully-active heterotetrameric holoenzyme. *Biochim Biophys Acta* **1164**: 223–225.

Middelhaufe S, Garzia L, Ohndorf UM, Kachholz B, Zollo M, Steegborn C. (2007). Domain mapping on the human metastasis regulator protein h-prune reveals a C-terminal dimerization domain. *Biochem J* **407**: 199–205.

Mocan I, Georgescauld F, Gonin P, Thoraval D, Cervoni L, Giartosio A *et al*. (2007). Protein phosphorylation corrects the folding defect of the neuroblastoma (S120G) mutant of human nucleoside diphosphate kinase A/Nm23-H1. *Biochem J* **403**: 149–156.

Otsuki Y, Tanaka M, Yoshii S, Kawazoe N, Nakaya K, Sugimura H. (2001). Tumor metastasis suppressor nm23H1 regulates Rac1 GTPase by interaction with Tiam1. *Proc Natl Acad Sci USA* **98**: 4385–4390.

Pagano MA, Meggio F, Ruzzene M, Andrzejewska M, Kazimierczuk Z, Pinna LA. (2004). 2-Dimethylamino-4,5,6,7-tetrabromo-1H-benzimidazole: a novel powerful and selective inhibitor of protein kinase CK2. *Biochem Biophys Res Commun* **321**: 1040–1044.

Palacios F, Schweitzer JK, Boshans RL, D'Souza-Schorey C. (2002). ARF6-GTP recruits Nm23-H1 to facilitate dynamin-mediated endocytosis during adherens junctions disassembly. *Nat Cell Biol* **4**: 929–936.

Rena G, Bain J, Elliott M, Cohen P. (2004). D4476, a cell-permeant inhibitor of CK1, suppresses the site-specific phosphorylation and nuclear exclusion of FOXO1a. *EMBO Rep* **5**: 60–65.

Reymond A, Volorio S, Merla G, Al-Maghtheh M, Zuffardi O, Bulfone A *et al*. (1999). Evidence for interaction between human PRUNE and nm23-H1 NDPKinase. *Oncogene* **18**: 7244–7252.

Steeg PS. (2005). New insights into the tumor metastatic process revealed by gene expression profiling. *Am J Pathol* **166**: 1291–1294.

Steeg PS, Bevilacqua G, Pozzatti R, Liotta LA, Sobel ME. (1988). Altered expression of NM23, a gene associated with low tumor metastatic potential, during adenovirus 2 Ela inhibition of experimental metastasis. *Cancer Res* **48**: 6550–6554.

Tseng YH, Vicent D, Zhu J, Niu Y, Adeyinka A, Moyers JS *et al*. (2001). Regulation of growth and tumorigenicity of breast cancer cells by the low molecular weight GTPase Rad and nm23. *Cancer Res* **61**: 2071–2079.

Wagner PD, Steeg PS, Vu ND. (1997). Two-component kinase-like activity of nm23 correlates with its motility-suppressing activity. *Proc Natl Acad Sci USA* **94**: 9000–9005.

Zhang B, Zhang Y, Shacter E. (2004). Rac1 inhibits apoptosis in human lymphoma cells by stimulating Bad phosphorylation on Ser-75. *Mol Cell Biol* **24**: 6205–6214.

Zollo M, Andre A, Cossu A, Sini MC, D'Angelo A, Marino N *et al*. (2005). Overexpression of h-prune in breast cancer is correlated with advanced disease status. *Clin Cancer Res* **11**: 199–205.

Supplementary Information accompanies the paper on the Oncogene website (http://www.nature.com/onc).